Thermal Transport in the Kitaev Model

Joji Nasu,[1] Junki Yoshitake,[2] and Yukitoshi Motome[2]
[1]Department of Physics, Tokyo Institute of Technology, Meguro, Tokyo 152-8551, Japan
[2]Department of Applied Physics, University of Tokyo, Bunkyo, Tokyo 113-8656, Japan
(Received 30 March 2017; revised manuscript received 2 June 2017; published 22 September 2017)

In conventional insulating magnets, heat is carried by magnons and phonons. In contrast, when the magnets harbor a quantum spin liquid state, emergent quasiparticles from the fractionalization of quantum spins can carry heat. Here, we investigate unconventional thermal transport yielded by such exotic carriers, in both longitudinal and transverse components, for the Kitaev model, whose ground state is exactly shown to be a quantum spin liquid with fractional excitations described as itinerant Majorana fermions and localized Z_2 fluxes. We find that the longitudinal thermal conductivity exhibits a single peak at a high temperature, while the nonzero frequency component has a peak at a low temperature, reflecting the spin fractionalization. On the other hand, we show that the transverse thermal conductivity is induced by the magnetic field in a wide temperature range up to the energy scale of the bare exchange coupling; while increasing temperature, the transverse response divided by temperature decreases from the quantized value expected for the topologically nontrivial ground state and shows nonmonotonic temperature dependence. These characteristic behaviors provide experimentally accessible evidence of fractional excitations in the proximity to the Kitaev quantum spin liquid.

DOI: 10.1103/PhysRevLett.119.127204

Insulating magnets provide a paradigmatic playground for quantum many-body effects in the spin degree of freedom of electrons in solids. In conventional magnets, the elementary excitation is known as magnons which describe the collective modes associated with long-range magnetic orders. Once the ordering is suppressed by strong quantum fluctuations, however, the magnets may possess exotic excitations yielded by the quantum many-body effects. Fractional quasiparticles in quantum spin liquids (QSLs), where any spontaneous symmetry breaking does not appear even at zero temperature (T), are archetypal examples of such exotic excitations [1,2]. For instance, in the celebrated resonating-valence-bond state, the low-energy excitations are described by spinons, spin-1/2 fermionic quasiparticles, which may bring about an emergent Fermi surface despite insulating magnets [3,4]. Considerable efforts have been devoted to experimental observation of such itinerant nature, e.g., in the low-T behavior of the specific heat and the thermal transport [5–7]. Nevertheless, identifying the fractionalization remains elusive because of obstacles in experiments and the lack of detailed theoretical information.

Recently, a quantum spin model, whose ground state is exactly shown to be a QSL, was proposed by Kitaev [8]. The elementary excitations in the Kitaev QSL are described by two types of quasiparticles emergent from the fractionalization of quantum spins: itinerant Majorana fermions and localized Z_2 fluxes. Moreover, it was pointed out that this Kitaev model may give a good description of spin-orbital entangled magnets [9], such as A_2IrO_3 (A = Li, Na) and α-$RuCl_3$. On this basis, precursors of the Kitaev QSL have been investigated in these materials, e.g., by the neutron and Raman scattering measurements [10,11], in comparison with the theoretical calculations [12–17]. Very recently, some attempts have been made to grasp the itinerant nature of the Majorana fermions by measuring the thermal conductivity [18–20]. While theoretical works have been done for the thermal transport in one-dimensional Kitaev systems [21,22] and that carried by magnons in magnetically ordered states in the Kitaev-Heisenberg model [23], the thermal conductivity owing to the Majorana fermions emergent in the two-dimensional Kitaev QSL remains unclear. Furthermore, an applied magnetic field can change the topology of the Majorana fermion states [8], which may lead to the quantized transverse conductivity in the low-T limit. Thus, theoretical inputs are highly desired for the thermal transport in both longitudinal and transverse components for the Kitaev model as a canonical reference.

In this Letter, we investigate the thermal transport originating from the emergent fractional quasiparticles in the Kitaev model. Using quantum Monte Carlo (QMC) simulations, we calculate the T dependences of both longitudinal and transverse thermal conductivities, with and without the weak magnetic field. We find that, in the absence of the magnetic field, the longitudinal zero-(nonzero-)frequency component exhibits a broad peak around the higher- (lower-)T peak of the specific heat. In an applied magnetic field, we show that, while the longitudinal component remains intact, the transverse component is induced in a wide T range; the latter divided by T shows nonmonotonic T dependence with rapidly approaching a quantized value at low T. We discuss these

peculiar behaviors from the viewpoint of thermal excitations of the fractional quasiparticles.

We consider the Kitaev model in an external magnetic field applied perpendicular to the honeycomb plane. The spin axis is taken by following Ref. [9] so as to be relevant to candidate materials like A_2IrO_3 ($A = Li$, Na) and α-$RuCl_3$. The Hamiltonian is given by

$$\mathcal{H} = -J \sum_{\gamma=x,y,z} \sum_{\langle jj' \rangle_\gamma} S_j^\gamma S_{j'}^\gamma - h \sum_j (S_j^x + S_j^y + S_j^z), \quad (1)$$

where $\langle jj' \rangle_\gamma$ represents a nearest-neighbor pair on one of three sets of inequivalent bonds, $\boldsymbol{S}_j = (S_j^x, S_j^y, S_j^z)$ is an $S = 1/2$ operator at position $\boldsymbol{r}_j$, J is the exchange constant assumed to be isotropic for three types of bonds, and h represents the magnetic field strength; see the inset of Fig. 1(d). In the absence of the magnetic field ($h = 0$), the ground state of the Kitaev model is exactly obtained by introducing itinerant Majorana fermions and localized Z_2 fluxes W_p, the latter of which are defined for each hexagonal plaquette p on the honeycomb lattice [8]. The ground state is given by all $W_p = +1$ (flux-free state), and

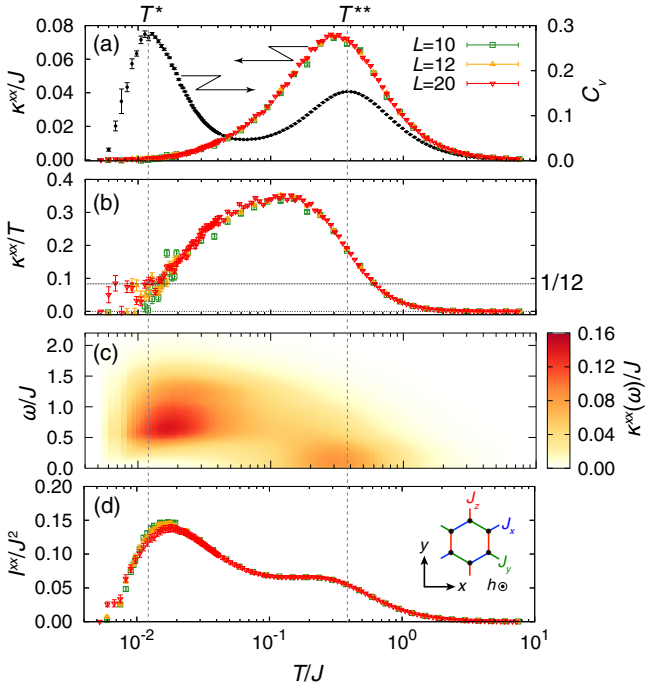

FIG. 1. (a) Longitudinal thermal conductivity, $\kappa^{xx} = \lim_{\omega\to 0}\kappa^{xx}(\omega)$ and (b) κ^{xx}/T as functions of T. In (a), we also plot the specific heat C_v for $L = 20$. T^* and T^{**} are two crossover temperatures, determined from the broad peaks in C_v. (c) Contour map of $\kappa^{xx}(\omega)$ on the T-ω plane calculated for the $L = 20$ cluster. (d) Integrated intensity $I^{xx} = \int_0^\infty \kappa^{xx}(\omega)d\omega$. The inset of (d) represents the honeycomb lattice on the xy plane where the Kitaev model is defined in an applied magnetic field h along the z direction [Eq. (1)]. The different bond colors illustrate three different types of bonds in the Kitaev model.

the system is in a gapless QSL phase where the itinerant Majorana fermion spectrum forms the massless Dirac nodes. In contrast, there is a nonzero gap $\Delta \sim 0.065J$ in the excitation of the localized Z_2 fluxes.

When h is small enough compared to Δ, one can derive an effective model by using the third-order perturbation, whose Hamiltonian is given by [8]

$$\tilde{\mathcal{H}} = -J \sum_{\gamma=x,y,z} \sum_{\langle jj' \rangle_\gamma} S_j^\gamma S_{j'}^\gamma - \tilde{h} \sum_{[jj''j']_{\alpha\beta\gamma}} S_j^\alpha S_{j''}^\beta S_{j'}^\gamma, \quad (2)$$

where the effective magnetic field $\tilde{h} \sim h^3/\Delta^2$; $[jj''j']_{\alpha\beta\gamma}$ represents three neighboring sites, where the neighboring pair jj'' ($j''j'$) are located on an α (γ) bond and β is taken to be neither α nor γ. The Hamiltonian $\tilde{\mathcal{H}}$ is exactly soluble for all $\tilde{h}$, while $\mathcal{H}$ in Eq. (1) is not for $h \neq 0$ [8]. This is shown, e.g., by introducing two kinds of Majorana fermions c_j and $\bar{c}_j$ [24–26], which enable us to rewrite the Hamiltonian into a bilinear form in terms of c_i as $\tilde{\mathcal{H}} = \frac{1}{2}\sum_{jj'} c_j A_{jj'}(\{\eta_b\}) c_j$; $A(\{\eta_b\})$ is a pure-imaginary Hermite matrix dependent on $\eta_b = i\bar{c}_j\bar{c}_{j'}$, which is a Z_2 conserved quantity taking ± 1 on the z bond $b = \langle jj' \rangle_z$ [27]. The flux in the plaquette p is given by $W_p = \eta_{b_1}\eta_{b_2}$, where b_1 and b_2 are the z bonds included in the hexagon p. The three-spin term in Eq. (2) turns into second-neighbor hopping of c_j in the bilinear Hamiltonian. Interestingly, this hopping term opens a gap in the Dirac spectrum of the Majorana fermion system and yields a chiral edge mode within the gap [8], similar to the Haldane model showing the quantum anomalous Hall effect in a zero magnetic field [28]. This topological nature was confirmed for the original model in Eq. (1) [29]. We note that, in addition to the second term in Eq. (2), the third-order perturbation in terms of h leads to another three-spin interaction described by interactions between the Majorana fermions c, which is supposed be irrelevant to the Dirac gap opening and omitted in the following analysis [8,30].

The bilinear Majorana representation for Eq. (2) allows us to perform QMC simulations without the negative sign problem [15,31,32]. To evaluate the thermal conductivity, we introduce the energy polarization operator defined as $\boldsymbol{P}_E = \sum_{jj'}[(\boldsymbol{r}_j + \boldsymbol{r}_{j'})/2]\tilde{\mathcal{H}}_{jj'}$, where $\tilde{\mathcal{H}}_{jj'} = \frac{1}{2} c_j A_{jj'} c_{j'}$ [33]. We set the Boltzmann constant k_B and the reduced Planck constant $\hbar$ to be unity. The energy current is introduced as $\boldsymbol{J}_E = (d\boldsymbol{P}_E/dt) = i[\tilde{\mathcal{H}}, \boldsymbol{P}_E]$. Note that $\boldsymbol{J}_E$ includes not only $\{c_j\}$ but also $\{\eta_b\}$ in the Majorana fermion representation [27]. In the Majorana fermion system, as the chemical potential is always fixed to zero regardless of the configuration of $\{\eta_b\}$, the energy current is equivalent to the heat current $\boldsymbol{J}_Q$. The thermal conductivity $\kappa^{\mu\nu}$ ($\mu, \nu = x, y$) is obtained by using the Kubo formula as $\kappa^{\mu\nu}_{\mathrm{Kubo}}(\omega) = (1/TV)\int_0^\infty dt e^{i(\omega+i\delta)t}\int_0^\beta d\lambda \langle J_Q^\mu(-i\lambda) J_Q^\nu(t)\rangle$, where $J_Q^\mu(t) = e^{i\tilde{\mathcal{H}}t} J_Q^\mu e^{-i\tilde{\mathcal{H}}t}$, $\beta = 1/T$ is the inverse temperature, V is the

volume of the system, and δ is a positive infinitesimal constant. While the longitudinal component is simply given by $\kappa^{\mu\mu}(\omega) = \kappa^{\mu\mu}_{\rm Kubo}(\omega)$, the transverse component $\kappa^{\mu\nu}(\omega)$ needs a contribution from "the gravitational magnetization" in addition to $\kappa^{\mu\nu}_{\rm Kubo}(\omega)$ [34,35]. We calculate $\kappa^{\mu\nu}(\omega)$ on the 30×30 superlattice of the $2L^2$-site cluster with configurations of $\{\eta_r\}$ generated by the QMC simulations [36,37]: we take 300 samples from the 40 000 MC steps after 10 000 MC steps for thermalization. The details of the calculation are given in the Supplemental Material [27].

First, we examine the longitudinal component of the thermal conductivity $\kappa^{xx}(=\kappa^{yy})$ in the absence of a magnetic field $\tilde{h} = 0$. Figure 1(a) shows the T dependence of $\kappa^{xx} = \lim_{\omega\to 0}\kappa^{xx}(\omega)$ [27]. We also display the specific heat C_v in Fig. 1(a). C_v has two broad peaks at $T^* \simeq 0.012J$ and $T^{**} \simeq 0.375J$ due to thermal fractionalization [32]: the low-T crossover at T^* comes from the release of a half of ln2 entropy related to the localized Z_2 fluxes W_p, while the high-T one at T^{**} is by the rest half from the itinerant Majorana fermions. In contrast, we find that κ^{xx} exhibits only a single broad peak near T^{**}. The result is far from the conventional wisdom that predicts $\kappa^{xx} \propto C_v$. This discrepancy is a direct consequence of the thermal fractionalization of quantum spins. Among the fractional quasiparticles, only the itinerant Majorana fermions can carry heat. Hence, κ^{xx} has a substantial contribution only near T^{**} where the itinerant Majorana fermions release their entropy.

We also present κ^{xx}/T in Fig. 1(b). As decreasing T, this quantity increases from zero around T^{**}, and decreases with approaching T^* after showing a broad hump at $T \sim 0.1J$. Below T^*, κ^{xx}/T appears to approach $\sim 1/12$, although the size dependence and statistical errors become comparatively large. The asymptotic behavior might be related to the minimum conductivity in graphene with disorder [38,39], as thermally excited Z_2 fluxes are regarded as scatterers for the itinerant Majorana fermions moving on the honeycomb lattice [40]. We note that the thermal conductivity by Majorana fermions is halved from that by electrons [34], leading to the asymptotic behavior $\kappa^{xx} \sim T/12$ as predicted in Ref. [43].

Figure 1(c) shows the contour map of $\kappa^{xx}(\omega)$ on the T-ω plane. $\kappa^{xx}(\omega)$ has a low-ω weight around T^{**}, which gives the peak of the $\omega \to 0$ limit, i.e., κ^{xx} in Fig. 1(a). On the other hand, the weight is shifted to a higher-ω region as lowering T, and enhanced to form a broad peak at $\omega \sim J$ around T^*. This might be related to the T dependence of the Majorana fermion density of states [27,32]. The weight is reduced rapidly for further lowering T below T^*. We note that $\kappa^{xx}(\omega)$ completely vanishes at $T = 0$ as the Kitaev Hamiltonian commutes with the energy current in the flux-free ground state owing to the particle-antiparticle equivalence of Majorana fermions [27]. We plot the integrated thermal conductivity defined by $I^{xx} = \int_0^\infty \kappa^{xx}(\omega)d\omega$ in Fig. 1(d) as a measure of the finite-ω response. As increasing T from $T = 0$, I^{xx} rapidly grows from zero and forms a broad peak around T^* originating from the contribution at $\omega \sim J$ of $\kappa^{xx}(\omega)$, while it decreases in the higher-T region after showing a shoulder around T^{**}. Thus, the nonzero-frequency thermal response is a good measure for a proliferation of localized Z_2 fluxes at $T \simeq T^*$. This counterintuitive result is attributed to a modulation of the itinerant Majorana fermion state by the coupling to thermally excited fluxes.

Next, we show the results in the presence of the magnetic field in Fig. 2. Here, we consider the weak $\tilde{h}$ range in Eq. (2) where the field-induced Majorana gap is smaller than the flux gap [27]. In this range of $\tilde{h}$, the double-peak structure of C_v hardly changes [27], and hence, we indicate T^* and T^{**} for $\tilde{h} = 0$ in Fig. 2. Similarly, the longitudinal thermal conductivity κ^{xx} is also almost unchanged by $\tilde{h}$ as shown in Fig. 2(a) [27], while the effect of $\tilde{h}$ is seen in the low-T behavior of κ^{xx}/T, as shown in Fig. 2(b): κ^{xx}/T at $T \to 0$ vanishes, reflecting the Dirac gap in the Majorana spectrum for nonzero $\tilde{h}$.

On the other hand, the magnetic field gives rise to a drastic response in a wider T range in the transverse thermal conductivity κ^{xy}. As mentioned above, in the gapped

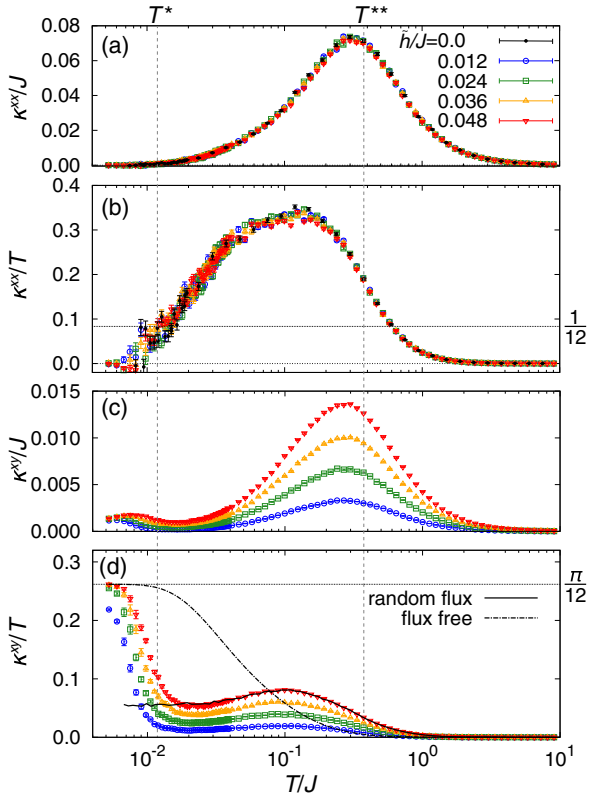

FIG. 2. (a) κ^{xx}, (b) κ^{xx}/T, (c) κ^{xy}, and (d) κ^{xy}/T in the magnetic field $\tilde{h}$. The data are calculated for $L = 8$, 10, and 12, but we show only the data for $L = 12$ as they are indistinguishable within the statistical errors. In (d), we also plot κ^{xy}/T calculated for the flux-free (dashed-dotted curve) and random flux (solid curve) cases at $\tilde{h}/J = 0.048$.

ground state for nonzero $\tilde{h}$, the system has a chiral edge mode inside the gap, which may lead to nontrivial topological phenomena such as off-diagonal transport [8], as in the massive Dirac fermion systems [44]. Here, we compute the $\tilde{h}$ and T dependence of κ^{xy} [Fig. 2(c)]. Note that κ^{xy} is directly obtained without any extrapolation in terms of ω, in contrast to κ^{xx} [27]. We find that $\tilde{h}$ induces κ^{xy} in a wide T range up to $T \sim J$, showing a broad peak around T^{**} similar to κ^{xx}. However, the $\tilde{h}$ dependence of κ^{xy} is distinct from that of κ^{xx}; the peak is enhanced by the magnetic field continuously from $\tilde{h} = 0$.

Remarkably, κ^{xy} shows a nonmonotonic T dependence, as more clearly displayed by κ^{xy}/T in Fig. 2(d); while decreasing T, κ^{xy}/T increases from zero around T^{**}, and shows a hump at $T \sim 0.1J$ similar to κ^{xx}/T in Fig. 2(b), but eventually, it arises again and converges a quantized value $\pi/12$ as $T \to 0$. The asymptotic value $\pi/12$ is derived from the edge current predicted in Ref. [8], which corresponds to a half of the quantized thermal Hall coefficient in conventional Chern insulators [34,35]. The low-T plateau of κ^{xy}/T is supported by the flux gap, and the deviation while raising T is caused by the Majorana fermions activated by thermally excited fluxes [27]. In Fig. 2(d), we compare the QMC data with those for the flux-free state (all $W_p = +1$) and the random W_p configuration at $\tilde{h} = 0.048J$. For the latter, we evaluate κ^{xy}/T from 10^3 random configurations of $\{\eta_b\}$. When we assume the flux-free configuration, κ^{xy}/T monotonically decreases from the quantized value with increasing T. The QMC result deviates from this behavior with a more rapid decrease around T^* where the Z_2 fluxes are thermally proliferated, as shown in Fig. 2(d). On the other hand, for the random configuration, κ^{xy}/T shows a hump around $T/J \sim 0.1$, which well accounts for the QMC data. This analysis clearly indicates that the nonmonotonic T dependence of κ^{xy}/T is yielded by thermal excitation of Z_2 fluxes from the flux-free topological ground state. In particular, the rapid decrease and the dip formation around T^* reflect the proliferation of Z_2 fluxes [27].

We show the field dependence of the longitudinal and transverse components of the thermal conductivity in Fig. 3, which are even and odd functions of $\tilde{h}$, respectively. Although κ^{xx}/T does not strongly depend on $\tilde{h}$ as shown in Fig. 3(a), κ^{xy}/T increases linearly to $\tilde{h}$ in the small $\tilde{h}$ region, and saturates to the quantized value $\pi/12$ for a large magnetic field, as shown in Fig. 3(b). While decreasing T, the slope increases and the saturation field decreases, and finally, $\kappa^{xy}/T = \mathrm{sgn}(\tilde{h})\pi/12$ at $T = 0$ [8,34]. The low-field behavior indicates that $\kappa^{xy}/T \propto h^3$, where h is the magnetic field in the original Hamiltonian in Eq. (1). The peculiar h dependence is one of the striking features in the unconventional thermal Hall effect in the paramagnetic state proximate to the QSL.

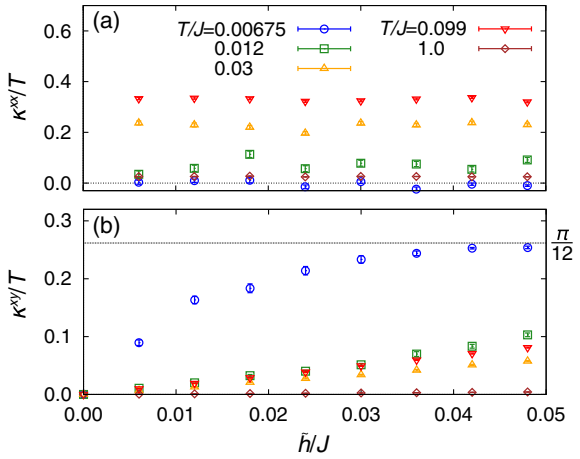

FIG. 3. $\tilde{h}$ dependences of (a) κ^{xx}/T and (b) κ^{xy}/T at several T for the $L = 12$ cluster.

Finally, we discuss the relevance of our results to Kitaev candidate materials, such as $A_2\mathrm{IrO}_3$ (A = Li and Na) and α-RuCl_3. Although these materials exhibit a magnetic order below $T_N \sim 10$ K [45,46], the Kitaev interaction has a much larger energy scale compared to T_N [10,47–51]: the low-T magnetic order is considered to appear due to small additional interactions. Therefore, the present results will be compared with the experimental data in the paramagnetic state above T_N where the magnetic properties are expected to be dominated by the Kitaev interaction. For instance, the high-T anomalous contribution in κ^{xx} observed in α-RuCl_3 [18] is likely consistent with our results. Although it might be difficult to experimentally distinguish the magnetic contribution from others such as phonons, recent experiments for other QSL candidates indicate that the phonon contribution is significantly small in κ^{xy} [7,52]. Thus, a nonzero κ^{xy} up to well above T_N will be more compelling evidence for the fractional excitations: the nonmonotonic T dependence of κ^{xy}/T comparable to the quantized value as well as the h^3 dependence is a direct consequence of the presence of the Majorana chiral edge mode and the thermal fluctuation of the Z_2 fluxes intrinsic in Kitaev physics.

In summary, we have investigated the thermal transport in the Kitaev model at finite T with and without an applied magnetic field using QMC simulations. We found that both longitudinal and transverse conductivities provide good probes for fractional quasiparticles, itinerant Majorana fermions and localized Z_2 fluxes, inherent to the Kitaev QSL. The $\omega = 0$ component of the longitudinal thermal conductivity exhibits a single peak structure around T^{**}, which is attributed to the itinerant Majorana fermions, while the dynamical component is enhanced around T^* due to the proliferation of the fluxes. In the presence of the magnetic field, the transverse component becomes nonzero and the transverse thermal conductivity divided by T exhibits a hump below T^{**}, and rapidly approaches a

quantized value in the low-T limit. We revealed that this peculiar T dependence is due to thermally excited Z_2 fluxes and the gapped Majorana spectrum in the magnetic field. Moreover, we found that the transverse conductivity is induced proportional to the third order of the magnetic field, while the longitudinal one is almost unchanged by the magnetic field. To our knowledge, the results provide the first quantitative theory for the thermal transport in the Kitaev model at finite T, which will be useful for the identification of QSL signatures in Kitaev candidate materials.

The authors thank W. Brenig, E.-G. Moon, and K. Nomura for helpful discussions and also thank Y. Kato for a critical reading of our manuscript. This work is supported by Grant-in-Aid for Scientific Research under Grants No. JP15K13533, No. JP16H00987, No. JP16K17747, and No. JP16H02206. Parts of the numerical calculations were performed in the supercomputing systems in ISSP, the University of Tokyo.

[1] X. G. Wen, Phys. Rev. B **44**, 2664 (1991).
[2] G. Misguich, in *Introduction to Frustrated Magnetism*, edited by C. Lacroix, P. Mendels, and F. Mila (Springer, Heidelberg, 2011), Chap. 16.
[3] P. W. Anderson, Mater. Res. Bull. **8**, 153 (1973).
[4] P. Fazekas and P. W. Anderson, Philos. Mag. **30**, 423 (1974).
[5] M. Yamashita, N. Nakata, Y. Senshu, M. Nagata, H. M. Yamamoto, R. Kato, T. Shibauchi, and Y. Matsuda, Science **328**, 1246 (2010).
[6] T. Isono, H. Kamo, A. Ueda, K. Takahashi, M. Kimata, H. Tajima, S. Tsuchiya, T. Terashima, S. Uji, and H. Mori, Phys. Rev. Lett. **112**, 177201 (2014).
[7] D. Watanabe, K. Sugii, M. Shimozawa, Y. Suzuki, T. Yajima, H. Ishikawa, Z. Hiroi, T. Shibauchi, Y. Matsuda, and M. Yamashita, Proc. Natl. Acad. Sci. U.S.A. **113**, 8653 (2016).
[8] A. Kitaev, Ann. Phys. (Amsterdam) **321**, 2 (2006).
[9] G. Jackeli and G. Khaliullin, Phys. Rev. Lett. **102**, 017205 (2009).
[10] A. Banerjee, C. Bridges, J.-Q. Yan, A. Aczel, L. Li, M. Stone, G. Granroth, M. Lumsden, Y. Yiu, J. Knolle *et al.*, Nat. Mater. **15**, 733 (2016).
[11] L. J. Sandilands, Y. Tian, K. W. Plumb, Y.-J. Kim, and K. S. Burch, Phys. Rev. Lett. **114**, 147201 (2015).
[12] J. Knolle, D. L. Kovrizhin, J. T. Chalker, and R. Moessner, Phys. Rev. Lett. **112**, 207203 (2014).
[13] J. Knolle, G.-W. Chern, D. L. Kovrizhin, R. Moessner, and N. B. Perkins, Phys. Rev. Lett. **113**, 187201 (2014).
[14] Y. Yamaji, T. Suzuki, T. Yamada, S. I. Suga, N. Kawashima, and M. Imada, Phys. Rev. B **93**, 174425 (2016).
[15] J. Nasu, J. Knolle, D. L. Kovrizhin, Y. Motome, and R. Moessner, Nat. Phys. **12**, 912 (2016).
[16] X.-Y. Song, Y.-Z. You, and L. Balents, Phys. Rev. Lett. **117**, 037209 (2016).
[17] J. Yoshitake, J. Nasu, and Y. Motome, Phys. Rev. Lett. **117**, 157203 (2016).
[18] D. Hirobe, M. Sato, Y. Shiomi, H. Tanaka, and E. Saitoh, Phys. Rev. B **95**, 241112 (2017).
[19] I. A. Leahy, C. A. Pocs, P. E. Siegfried, D. Graf, S.-H. Do, K.-Y. Choi, B. Normand, and M. Lee, Phys. Rev. Lett. **118**, 187203 (2017).
[20] R. Hentrich, A. U. B. Wolter, X. Zotos, W. Brenig, D. Nowak, A. Isaeva, T. Doert, A. Banerjee, P. Lampen-Kelley, D. G. Mandrus, S. E. Nagler, J. Sears, Y.-J. Kim, B. Büchner, and C. Hess, arXiv:1703.08623.
[21] R. Steinigeweg and W. Brenig, Phys. Rev. B **93**, 214425 (2016).
[22] A. Metavitsiadis and W. Brenig, Phys. Rev. B **96**, 041115 (2017).
[23] G. L. Stamokostas, P. E. Lapas, and G. A. Fiete, Phys. Rev. B **95**, 064410 (2017).
[24] H.-D. Chen and J. Hu, Phys. Rev. B **76**, 193101 (2007).
[25] X.-Y. Feng, G.-M. Zhang, and T. Xiang, Phys. Rev. Lett. **98**, 087204 (2007).
[26] H.-D. Chen and Z. Nussinov, J. Phys. A **41**, 075001 (2008).
[27] See Supplemental Material at http://link.aps.org/supplemental/10.1103/PhysRevLett.119.127204 for the formulation of the thermal conductivity in the Majorana fermion representation and details of the calculations.
[28] F. D. M. Haldane, Phys. Rev. Lett. **61**, 2015 (1988).
[29] H.-C. Jiang, Z.-C. Gu, X.-L. Qi, and S. Trebst, Phys. Rev. B **83**, 245104 (2011).
[30] M. Hermanns, K. O'Brien, and S. Trebst, Phys. Rev. Lett. **114**, 157202 (2015).
[31] J. Nasu, M. Udagawa, and Y. Motome, Phys. Rev. Lett. **113**, 197205 (2014).
[32] J. Nasu, M. Udagawa, and Y. Motome, Phys. Rev. B **92**, 115122 (2015).
[33] H. Katsura, N. Nagaosa, and P. A. Lee, Phys. Rev. Lett. **104**, 066403 (2010).
[34] K. Nomura, S. Ryu, A. Furusaki, and N. Nagaosa, Phys. Rev. Lett. **108**, 026802 (2012).
[35] H. Sumiyoshi and S. Fujimoto, J. Phys. Soc. Jpn. **82**, 023602 (2013).
[36] H. Ishizuka and Y. Motome, Phys. Rev. B **88**, 100402 (2013).
[37] A. E. Antipov, Y. Javanmard, P. Ribeiro, and S. Kirchner, Phys. Rev. Lett. **117**, 146601 (2016).
[38] A. W. W. Ludwig, M. P. A. Fisher, R. Shankar, and G. Grinstein, Phys. Rev. B **50**, 7526 (1994).
[39] K. Ziegler, Phys. Rev. B **75**, 233407 (2007).
[40] The Wiedemann-Franz law is not violated in the present case with noninteracting Majorana fermions coupled with thermally fluctuating Z_2 fluxes, in contrast to interacting Dirac electron systems [41,42]. The presence of the minimum T-linear coefficient of the thermal conductivity was also discussed in the Majorana fermion system with long-range disorder [43], which indicates $\kappa^{xx}/T \sim 1/12$ in the low-T limit.
[41] A. Principi and G. Vignale, Phys. Rev. Lett. **115**, 056603 (2015).
[42] A. Lucas, J. Crossno, K. C. Fong, P. Kim, and S. Sachdev, Phys. Rev. B **93**, 075426 (2016).
[43] R. Nakai and K. Nomura, Phys. Rev. B **89**, 064503 (2014).

[44] K. Nomura and N. Nagaosa, Phys. Rev. Lett. **106**, 166802 (2011).
[45] Y. Singh and P. Gegenwart, Phys. Rev. B **82**, 064412 (2010).
[46] Y. Kubota, H. Tanaka, T. Ono, Y. Narumi, and K. Kindo, Phys. Rev. B **91**, 094422 (2015).
[47] J. Chaloupka, G. Jackeli, and G. Khaliullin, Phys. Rev. Lett. **110**, 097204 (2013).
[48] K. Foyevtsova, H. O. Jeschke, I. I. Mazin, D. I. Khomskii, and R. Valentí, Phys. Rev. B **88**, 035107 (2013).
[49] Y. Yamaji, Y. Nomura, M. Kurita, R. Arita, and M. Imada, Phys. Rev. Lett. **113**, 107201 (2014).
[50] V. M. Katukuri, S. Nishimoto, V. Yushankhai, A. Stoyanova, H. Kandpal, S. Choi, R. Coldea, I. Rousochatzakis, L. Hozoi, and J. van den Brink, New J. Phys. **16**, 013056 (2014).
[51] H.-S. Kim, V. Vijay Shankar, A. Catuneanu, and H.-Y. Kee, Phys. Rev. B **91**, 241110 (2015).
[52] K. Sugii, M. Shimozawa, D. Watanabe, Y. Suzuki, M. Halim, M. Kimata, Y. Matsumoto, S. Nakatsuji, and M. Yamashita, Phys. Rev. Lett. **118**, 145902 (2017).